Freely decaying turbulence in a finite domain at finite Reynolds number

Cite as: Phys. Fluids **32**, 095109 (2020); https://doi.org/10.1063/5.0015009
Submitted: 25 May 2020 . Accepted: 20 August 2020 . Published Online: 04 September 2020

Mohammad Anas, Pranav Joshi, and Mahendra K. Verma

Physics of Fluids ARTICLE scitation.org/journal/phf

Freely decaying turbulence in a finite domain at finite Reynolds number

Cite as: Phys. Fluids 32, 095109 (2020); doi: 10.1063/5.0015009
Submitted: 25 May 2020 • Accepted: 20 August 2020 •
Published Online: 4 September 2020

Mohammad Anas,[1,a] Pranav Joshi,[1,b] and Mahendra K. Verma[2,c]

AFFILIATIONS

[1] Department of Mechanical Engineering, Indian Institute of Technology, Kanpur 208016, India
[2] Department of Physics, Indian Institute of Technology, Kanpur 208016, India

[a] Author to whom correspondence should be addressed: anas@iitk.ac.in
[b] Electronic mail: jpranavr@iitk.ac.in
[c] Electronic mail: mkv@iitk.ac.in

ABSTRACT

We perform direct numerical simulations to study the effects of the finite Reynolds number and domain size on the decay law of Saffman turbulence. We observe that the invariant for Saffman turbulence, $u^2\ell^3$, and non-dimensional dissipation coefficient, $C_\epsilon = \epsilon/(u^3/\ell)$, are sensitive to finite domain size; here, u is the rms velocity, ℓ is the integral length scale, and ϵ is the energy dissipation rate. Consequently, the exponent n in the decay law $u^2 \sim t^{-n}$ for Saffman turbulence deviates from 6/5. Due to the finite Reynolds number and the domain size, Saffman turbulence decays at a faster rate (i.e., $n > 6/5$). However, the exponent $n = 6/5$ is more sensitive to the domain size than to the Reynolds number. From the simulations, we find that n remains close to 6/5 as long as $R_\lambda \gtrsim 10$ and $\ell \lesssim 0.3L_{box}$; here, R_λ is the Reynolds number based on the Taylor microscale and L_{box} is the domain size. We also notice that n becomes slightly lower than 6/5 for a part of the decay period. Interestingly, this trend $n < 6/5$ is also observed earlier in freely decaying grid-generated turbulence.

I. INTRODUCTION

Turbulence is a very complex phenomenon; many of its observed characteristics lack satisfactory explanations. Consider, for example, one of the most classical problems of turbulence—freely decaying grid-generated turbulence. It is clear that in freely decaying turbulence, the kinetic energy of turbulence decays with time due to viscous dissipation; however, there is no general agreement on its decay rate.[1] Although significant efforts have been made to understand the physics of freely decaying turbulence, it still remains one of the most debatable topics of turbulence.

Kolmogorov[2] was the first to propose the decay law for freely decaying turbulence. According to him, the decay of kinetic energy E of homogeneous isotropic turbulence with time t is independent of viscosity and follows a power-law $E \sim t^{-n}$ with the decay law exponent $n = 10/7$. Kolmogorov's predictions for freely decaying turbulence are based on the assumptions that during the decay of turbulence, the Loitsyansky integral $I = -\int r^2 \langle \mathbf{u}\cdot\mathbf{u}' \rangle d\mathbf{r}$ is invariant and the Saffman integral $L = \int \langle \mathbf{u}\cdot\mathbf{u}' \rangle d\mathbf{r} = 0$; here, $\mathbf{u}$ and $\mathbf{u}'$ are the velocities at two points separated by the displacement vector $\mathbf{r}$. The freely decaying turbulence with the Loitsyansky integral as an invariant is commonly known as Batchelor turbulence, which exhibits energy spectrum scaling $E(k) \sim k^4$ at large scales and $u^2\ell^5$ as an invariant, where k is the wavenumber, u is the rms velocity, and ℓ is the integral length scale. Combining $u^2\ell^5 = const.$ with the empirical relation for the energy dissipation rate, $\epsilon = C_\epsilon(u^3/\ell)$, we derive the power laws, $E \sim t^{-10/7}$ and $\ell \sim t^{2/7}$ for freely decaying Batchelor turbulence, where C_ϵ is a constant known as the non-dimensional dissipation coefficient. Note that the assumption that C_ϵ remains constant in freely decaying turbulence is valid only at high Reynolds numbers. At low or moderately high Reynolds number, C_ϵ changes with time in freely decaying turbulence.[3–7]

Saffman[8] disagreed with Kolmogorov's assumptions for freely decaying turbulence. He argued that in freely decaying turbulence, L is a non-zero invariant, whereas I is not an invariant. The type of turbulence in which L is non-zero and an invariant

is commonly known as Saffman turbulence, which exhibits $E(k) \sim k^2$ scaling at large scales and $u^2\ell^3$ as an invariant. Combining $u^2\ell^3 = const.$ with $\epsilon = C_\epsilon(u^3/\ell)$, we obtain the well-known power laws for freely decaying Saffman turbulence, $E \sim t^{-6/5}$ and $\ell \sim t^{2/5}$.

Both types of turbulence, Batchelor and Saffman, can be easily generated in direct numerical simulations (DNS).[1,9,10] However, experimental data of freely decaying grid-generated turbulence are more consistent with the characteristics of Saffman turbulence.[11–15] In a famous experiment of grid-generated turbulence, Comte-Bellot and Corrsin[11] obtained the decay law exponent $n \approx 6/5$, same as that for Saffman turbulence. Krogstad and Davidson[12] observed decay law exponent close to $n = 6/5$ for freely decaying grid generated turbulence and argued that Saffman turbulence is the most probable type for grid-generated turbulence. Morize and Moisy[15] also obtained $n \approx 6/5$ in the grid-generated turbulence by using PIV (particle image velocimetry) measurements. These results indicate that Saffman turbulence is more likely to manifest in grid-generated turbulence. In this work, we consider only Saffman turbulence for our analysis.

The implicit assumption in the discussed decay laws, $E \sim t^{-6/5}$ or $E \sim t^{-10/7}$, is that the Reynolds number of the turbulence remains high ($R_\lambda \gg 1$) throughout the decay period, and the turbulence is freely decaying in a large domain (i.e., $\ell \ll L_{box}$), where R_λ is the Reynolds number based on the Taylor microscale and L_{box} is the domain size. However, technological constraints in experiments and simulations restrict the study of freely decaying turbulence to a finite Reynolds number and in a finite domain.[1,13,16] Therefore, it is necessary to systematically assess the effects of finite Reynolds number and domain size on the decay laws to enable a fair comparison between the data obtained by using experiments, simulations, and theories. This is the focus of the present paper.

Using a phenomenological model, Skrbek and Stalp[16] studied the effect of finite domain size on freely decaying turbulence. They predicted that due to the saturation of growing large eddies in a finite domain, the decay law exponent n becomes higher than 6/5 in freely decaying turbulence. Using Eddy-Damped Quasi-Normal Markovian (EDQNM) model, Meldi and Sagaut[17] predicted the correction to be applied to the power-law exponent $n = 6/5$ due to the periodic boundary conditions in a finite domain. Thornber[18] studied the effect of finite domain size on freely decaying turbulence by using large eddy simulations (LES). He remarked that the exponent $m = 2/5$ in the power law $\ell \sim t^m$ for Saffman turbulence is more sensitive to the finite domain size than the decay law exponent $n = 6/5$. Davidson[1] and Meldi and Sagaut[17] prescribed that if the integral length scale ℓ remains less than one-tenth of the domain size L_{box} during the decay period, the effect of periodic boundary conditions on the decay law exponent would be insignificant. Additionally, the higher value n ($n > 6/5$) in decaying turbulent flow can intuitively be explained using the energy dissipation relation. For the saturated integral length scale ($\ell = const.$) in a finite domain, $\epsilon = C_\epsilon(u^3/\ell)$ predicts $E \sim t^{-2}$, a faster decay than that of Saffman turbulence ($E \sim t^{-6/5}$).

In this work, we assess some of the prior results and predictions on the effects of domain size and also study the effect of finite Reynolds number on the decay law of Saffman turbulence by using direct numerical simulations. This paper is organized as follows: We give details of the numerical simulations in Sec. II, discuss the results in Sec. III, and conclude our observations in Sec. IV.

II. SIMULATION DETAILS

We solve the Navier–Stokes equation,

$$\partial_t \mathbf{u} + (\mathbf{u}\cdot\nabla)\mathbf{u} = -\nabla p/\rho + \nu\nabla^2\mathbf{u} + \mathbf{f}, \tag{1}$$

$$\nabla\cdot\mathbf{u} = 0, \tag{2}$$

in Fourier space using a pseudo-spectral code Tarang[19,20] in a triply periodic box of size $L_{box} = 2\pi$. Here, $\mathbf{u}$ is the velocity field, p is the pressure field, and ρ and ν are the density and kinematic viscosity of the fluid, respectively. The forcing field $\mathbf{f}$ is set to zero for the freely decaying turbulence. For time integration, we use the fourth-order Runge–Kutta (RK4) method with time step Δt computed from the CFL (Courant–Friedrichs–Lewy) condition. We use the 2/3 rule for dealiasing.

For all the simulations (except one), we use the following form of the energy spectrum with random Gaussian noise, similar to that in the work of Ishida, Davidson, and Kaneda,[9] and fix the initial energy to unity,

$$E(k, t=0) \sim k^\sigma \exp(-(k/k_p)^2). \tag{3}$$

We name it *Synthetic* initial condition. Here, we set $\sigma = 2$ to obtain $E(k, t = 0) \sim k^2$ (Saffman turbulence) scaling at large scales, and wavenumber k_p, which corresponds to the size of large eddies, is varied to control the initial ℓ/L_{box}. In one of the simulations, we use a fully evolved and statistically stationary turbulence as an initial condition. We develop this flow field by applying a random forcing scheme that supplies constant energy and no kinetic helicity in the wavenumber band $k_f \in (11, 12)$.[21–24] We name it *evolved* initial condition. Interestingly, this turbulent flow also exhibits $E(k) \sim k^2$ scaling at large scales in the steady state. For all the simulations, $k_{max}\eta > 1$, ensuring that the grid spacing is sufficient to resolve the smallest scale of the flow, where k_{max} is the largest wavenumber in the simulations and η is the Kolmogorov length scale in the turbulent flow.

Table I presents the details of the simulations and the key results obtained for freely decaying Saffman turbulence. We perform seven simulations (S1–S7) with the *synthetic* initial condition and one simulation with the *evolved* (SF) initial condition for different k_p and ν to obtain a wide range of initial Reynolds numbers and ℓ/L_{box}. The Reynolds number based on the Taylor microscale for isotropic turbulence is defined as

$$R_\lambda = \frac{2}{3}\mathrm{E}\sqrt{\frac{15}{\nu\epsilon}}.$$

τ_i represents the initial transient period. We estimate τ_i by using the temporal variation of the decay law exponent n [Fig. 3(b)]. τ_i is defined as the time when $\partial n/\partial\tau$ first becomes equal to −0.01 after the initial maximum. μ_n and σ_n given in the table are mean and standard deviation of n, respectively, from $\tau = \tau_i$ to $\tau = \tau_f$, where τ_f is the time when $\ell/L_{box} \approx 0.3$. The values of R_λ in the table are at $\tau = 0$, $\tau = \tau_i$, and $\tau = \tau_f$. Note that the time τ is normalized by initial eddy turn-over time.

In Sec. III, we discuss the results obtained from the simulations.

TABLE I. Details of the simulations for Saffman turbulence with the synthetic and the evolved initial conditions. N is the number of grid points in each direction. R_λ are at $\tau = 0$, $\tau = \tau_i$, and $\tau = \tau_f$, respectively, and ℓ/L_{box} are at $\tau = 0$ and $\tau = \tau_i$; here, τ_f is the time where $\ell = 0.3L_{box}$. μ_n and σ_n are mean and standard deviation of n, respectively, from $\tau = \tau_i$ to $\tau = \tau_f$.

Runs	N	ν	k_p (k_f for SF)	τ_i	τ_f	R_λ	ℓ/L_{box}	$\mu_n \pm \sigma_n$
S1	512	0.001	5	5.1	6.3	320, 45, 44	0.219, 0.291	1.16 ± 0.005
S2	512	0.001	10	12.1	15.1	155, 29, 28	0.112, 0.281	1.10 ± 0.007
S3	512	0.001	20	14.9	49.7	76, 18, 17	0.056, 0.197	1.13 ± 0.009
S4	512	0.001	30	21.7	84.9	50, 13, 12	0.038, 0.177	1.17 ± 0.01
S5	512	0.001	40	21.1	154.1	38, 11, 9	0.028, 0.144	1.20 ± 0.01
S6	1024	0.0005	40	17.5	233.1	75, 17, 13	0.028, 0.111	1.21 ± 0.02
S7	1024	0.0005	80	23.4	500	37, 10, 7	0.014, 0.076	1.23 ± 0.005
SF	512	0.001	(11, 12)	15.1	81.8	46, 12, 10	0.069, 0.160	1.21 ± 0.03

III. RESULTS AND DISCUSSION

In this section, we discuss the results for freely decaying Saffman turbulence obtained by using the synthetic and evolved initial conditions.

Figure 1 shows the temporal variation of R_λ and ℓ/L_{box}. We observe that R_λ decreases, whereas ℓ increases with time. Runs S1 and S2 have relatively high Reynolds number and high initial ℓ/L_{box}, whereas S5 and S7 have relatively low Reynolds number and low initial ℓ/L_{box}. Among all the simulations, only S6 has both reasonably high R_λ and low ℓ/L_{box} at the same time throughout the decay period. Squares and circles marked in Fig. 1 at $\tau = \tau_i$ and $\tau = \tau_f$, respectively, indicate that as long as $\ell \lesssim 0.3L_{box}$, the growth of the integral length scale and the decay of the Reynolds number approximately follow the power laws, $\ell \sim \tau^{2/5}$ and $R_\lambda \sim \tau^{-1/10}$, respectively, for most of the runs. Later in the discussion, we also show that the effects of finite domain size on the decay law $E \sim \tau^{-6/5}$ are not significant as long as $\ell \lesssim 0.3L_{box}$ for Saffman turbulence.

Since the decay law for Saffman turbulence is the outcome of the assumed constancy of $u^2\ell^3$ and C_ϵ during the decay period, we need first to analyze their temporal variation. Figure 2 shows the variation of $u^2\ell^3$ and C_ϵ with time. We notice that both the quantities, $u^2\ell^3$ and C_ϵ, are not strictly constant during the decay period. Marked circles on the lines in Fig. 2(a) indicate that the

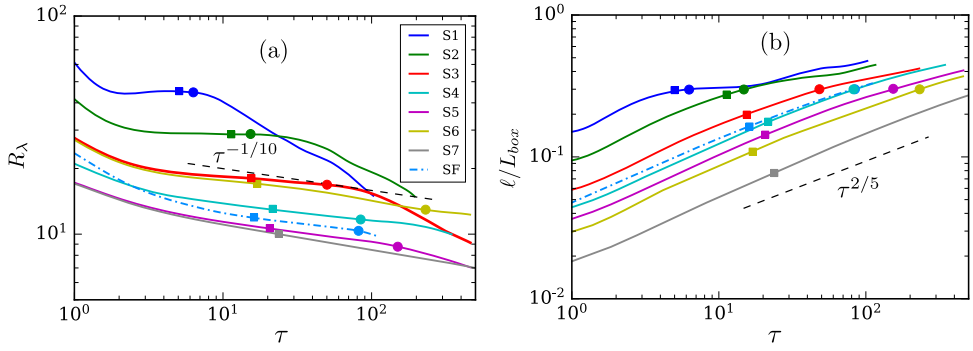

FIG. 1. Temporal variation of (a) R_λ and (b) ℓ/L_{box} for Saffman turbulence with the synthetic and the evolved initial conditions. Dashed lines in (a) and (b) represent the power laws for Saffman turbulence, $R_\lambda \sim \tau^{-1/10}$ and $\ell \sim \tau^{2/5}$, respectively. Marked squares and circles represent τ at which $\partial n/\partial\tau \approx -0.01$ and $\ell \approx 0.3L_{box}$, respectively.

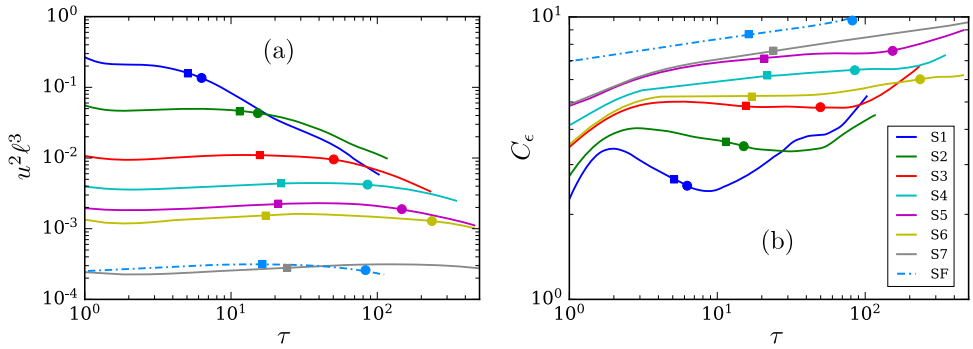

FIG. 2. Temporal variation of (a) $u^2\ell^3$ and (b) C_ϵ for Saffman turbulence with the synthetic and the evolved initial conditions. Marked squares and circles represent τ at which $\partial n/\partial\tau \approx -0.01$ and $\ell \approx 0.3L_{box}$, respectively.

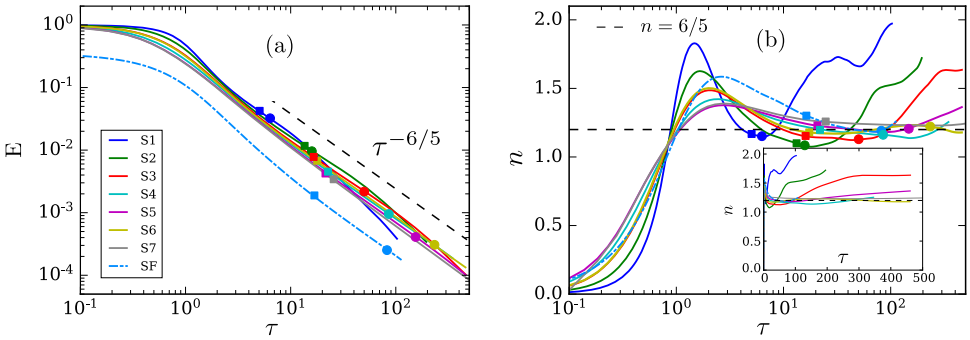

FIG. 3. (a) Decay of kinetic energy E and (b) the temporal variation of the associated decay law exponent n for freely decaying Saffman turbulence with the synthetic and the evolved initial conditions [inset in (b) shows time using a linear scale]. Marked squares and circles represent τ at which $\partial n/\partial\tau \approx -0.01$ and $\ell \approx 0.3L_{box}$, respectively. Dashed lines represent the decay law, $E \sim \tau^{-6/5}$ and $n = 6/5$ in (a) and (b), respectively.

deviation of $u^2\ell^3$ from constancy starts when ℓ becomes larger than $\sim 0.3L_{box}$ for most runs. The run S1, which has the highest ℓ/L_{box}, exhibits the maximum deviation of $u^2\ell^3$ and C_ϵ from their constancy. For the runs (S3–S6), which have reasonably high R_λ and low ℓ/L_{box}, C_ϵ remains almost constant throughout the decay period.

Figure 3 shows the decay of kinetic energy E and the variation of the associated decay law exponent n with time. We observe that the decay of turbulent flow first passes through a transient period. Interestingly, our simulations show that the transient period is inversely correlated with the initial Reynolds number. As the initial Reynolds number increases, the transient period decreases (see Table I), suggesting that τ_i could be some sort of relaxation time in decaying turbulent flow. As expected, the effect of the non-constancy of $u^2\ell^3$ and C_ϵ with time directly is reflected on the decay law of kinetic energy; the exponent n does not remain close to 6/5 throughout the decay period. The runs S1 and S2, which have relatively high ℓ/L_{box}, exhibit significant deviation from $n = 6/5$, and n is higher than 6/5 in these runs. For the rest of the runs (S3–S7 and SF), which have relatively low ℓ/L_{box}, n remains close to 6/5. Note that the run S7, which has the lowest ℓ/L_{box} and R_λ among all the simulations, shows n slightly higher than 6/5. The runs S5 and S6 with reasonably high R_λ and low ℓ/L_{box} at the same time exhibit exponent n closest to 6/5.

These observations suggest that the effect of finite domain size (e.g., the runs S1 and S2) and Reynolds number (e.g., the run S7) on freely decaying turbulence makes the decay faster (i.e., $n > 6/5$). This could be the main reason why experiments and simulations of freely decaying turbulence (with low R_λ and high ℓ/L_{box}) exhibit $n > 6/5$, and sometimes, the results are incorrectly interpreted to represent Batchelor turbulence ($n \approx 10/7$) due to the finite Reynolds number and domain size. Skrbek and Stalp[16] discussed this observation and argued that $n > 6/5$ observed in grid-generated turbulence is due to the saturation of growing large eddies in a finite domain. Thus, using the value of n ($n = 6/5$ and $n = 10/7$ for Saffman and Batchelor turbulence, respectively) is not a reliable way of distinguishing between Saffman and Batchelor turbulence.

Moreover, our simulations suggest that the effect of the finite domain size on the decay law is more, as compared to the effect of the finite Reynolds number. Also, for the simulations that have $\ell \lesssim 0.3L_{box}$, n remains close to 6/5 during the decay period. This observation suggests that the condition, $\ell \lesssim 0.1L_{box}$ prescribed by Davidson[1] and Meldi and Sagaut[17] to avert the effect of finite domain size, is perhaps over-restrictive; the condition $\ell \lesssim 0.3L_{box}$ may be sufficient to observe the decay law close to $E \sim \tau^{-6/5}$ for Saffman turbulence. A noticeable difference between the simulations with the synthetic and the evolved initial conditions is that the decay law exponent n for the run SF remains closer to 6/5 than that observed in the run S2, which has $k_p = 10$ [close to $k_f \in (11, 12)$]. This difference may be a result of the fact that S2 uses a synthetic initial condition, whereas SF employs a more realistic initial condition—an evolved turbulence.

For the runs S1–S6 and SF, we also observe that n becomes slightly lower than 6/5 for a part of the decay period. Interestingly, n slightly lower than 6/5 ($n \approx 1.1$) is also observed in many grid-generated turbulence experiments.[11,12,15] Krogstad and Davidson[12] argued that $n < 6/5$ in grid-generated turbulence arises due to the decay of C_ϵ with time in freely decaying turbulence. However, we observe $n < 6/5$, for a part of the decay period, also for the runs that exhibit increasing C_ϵ with time [see S4–S6 in Fig. 2(b)]. Therefore, the observation $n < 6/5$ in freely decaying grid-turbulence still appears to be an unsolved issue, and it requires further investigations.

Figure 4 shows the temporal variation of the energy dissipation rate ϵ. During the initial period, ϵ increases and reaches its peak. Yoffe and McComb[7] used this behavior of ϵ to estimate the initial

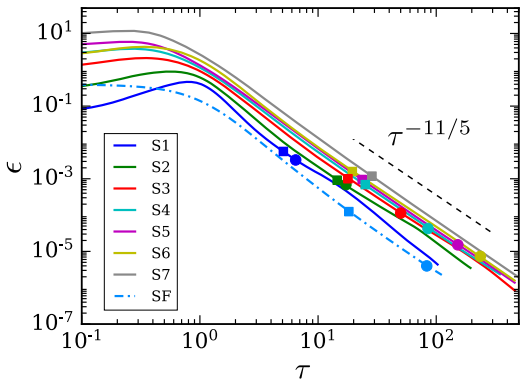

FIG. 4. Temporal variation of energy dissipation rate for Saffman turbulence with the synthetic and the evolved initial conditions. Note that during the initial period ϵ increases. Marked squares and circles represent τ at which $\partial n/\partial\tau \approx -0.01$ and $\ell \approx 0.3L_{box}$, respectively. Dashed line represents $\epsilon \sim \tau^{-11/5}$.

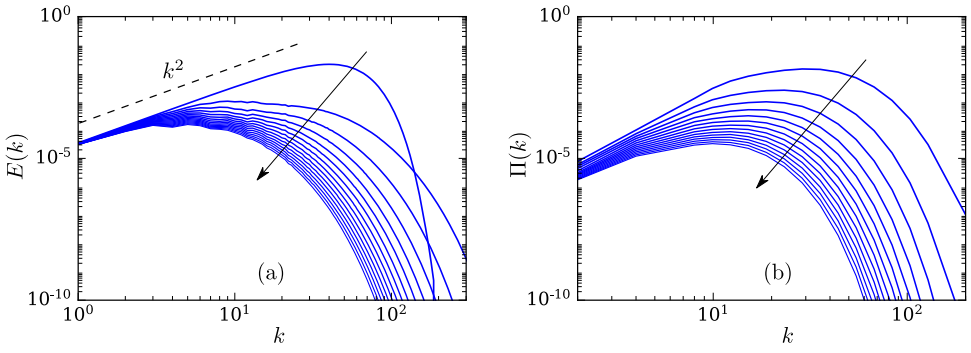

FIG. 5. Temporal variation of (a) energy spectrum from $\tau = 0$ to $\tau \approx 64.4$ and (b) energy flux from $\tau \approx 4.6$ to $\tau \approx 64.4$ with time difference $\Delta\tau \approx 4.6$ for the run S6. Note that the energy transfer remains forward. The directions of arrows indicate increasing time.

transient period. However, we employ initial temporal variation of n, instead of ϵ, to estimate τ_i, since the method of Yoffe and McComb[7] fails to estimate the transient period for the run SF. Unlike the runs with the synthetic initial conditions, the energy dissipation rate ϵ for the evolved initial condition (run SF) starts decreasing from $\tau = 0$. After the initial transient period, the decay of ϵ, as expected, exhibits a power law close to $\epsilon \sim \tau^{-11/5}$ for the runs having $\ell \lesssim 0.3L_{box}$.

Figure 5 shows the temporal variation of the energy spectrum and the flux for the run S6 (other simulations exhibit similar behavior). Temporal variation of the energy spectrum [Fig. 5(a)] shows that the energy of all the scales decays with time after the initial transient period. The energy flux $\Pi(k)$, which is the net transfer of energy out of the sphere of radius k by the modes inside the sphere,[25,26] remains positive with the decay of turbulence. It indicates that the energy transfer is forward (from large to small scales) throughout the decay period [see Fig. 5(b)]. Figure 6 exhibits shell to shell energy transfer in Fourier space. Shell to shell energy transfer is a useful tool to analyze whether the energy transfer is local or non-local in a turbulent flow.[25] Local energy transfer implies that a major fraction of energy is transferred to the neighboring modes, whereas non-local indicates that a significant amount of energy is also transferred to distant modes. In Fig. 6, $\mathcal{D}$ and $\mathcal{R}$ represent the donor and the receiver shells, respectively. For more details on the shell to shell energy transfer, see the work of Verma.[25] With these definitions, Fig. 6 shows that the energy transfer not only remains forward but also local in freely decaying turbulence.

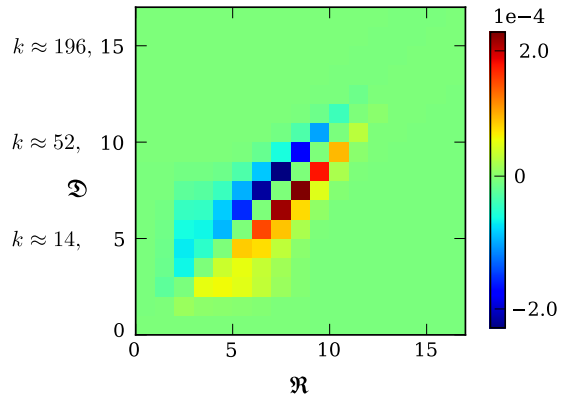

FIG. 6. Shell to shell energy transfer at $\tau \approx 18.4$ for the run S6. Shells $\mathfrak{D}$, $\mathfrak{R} = 5, 10$, and 15 correspond to wavenumbers $k \approx 14$, 52, and 196, respectively. Note that the energy transfer is forward and local.

IV. CONCLUSIONS

In this work, we study the effects of finite Reynolds number and domain size on the decay law of freely decaying Saffman turbulence by using direct numerical simulations. We observe that due to finite Reynolds number and domain size, the decay law exponent n becomes higher than that proposed for Saffman turbulence ($n = 6/5$). This could be the primary reason why $n > 6/5$ is frequently observed in experiments and simulations (with the finite Reynolds number and domain size) of freely decaying turbulence. Hence, the value of power law exponent n in any simulations or experiments is not a trustworthy way to distinguish between Saffman ($n = 6/5$) and Batchelor ($n = 10/7$) turbulence.

Furthermore, the effect of finite Reynolds numbers on the decay law exponent, $n = 6/5$, is relatively less as compared to that of finite domain size. Also, the effect of finite domain size on the decay law $E \sim t^{-6/5}$ is perhaps not as restrictive as that proposed earlier ($\ell \lesssim 0.1L_{box}$). Our simulations suggest that the conditions $R_\lambda \gtrsim 10$ and $\ell \lesssim 0.3L_{box}$ are sufficient to observe $n \approx 6/5$ in decaying Saffman turbulence. We also notice that the decay law exponent n becomes slightly lower than 6/5 for a part of the decay period. Interestingly, this trend $n < 6/5$ is also observed in earlier grid-generated turbulence experiments. These observations for freely decaying Saffman turbulence suggest that care must be taken while making any conclusive remarks from the data obtained from experiments and simulations at finite Reynolds number and in a finite domain.

We also perform a similar analysis for freely decaying Batchelor turbulence(not included in this paper). We use $\sigma = 4$ in Eq. (3) to ensure $E(k \to 0) \sim k^4$ scaling at $\tau = 0$ for the energy spectrum. Compared to Saffman turbulence, we observe a stronger dependence of the decay law exponent $n = 10/7$ for Batchelor turbulence on finite Reynolds numbers.

In this paper, we have only considered an idealized case of turbulence—incompressible homogeneous isotropic turbulence. However, finite Reynolds numbers and domain size may also play a crucial role and may affect the dynamics of decaying anisotropic and/or compressible turbulence. In a future study, it would be interesting to analyze the effects of finite Reynolds numbers and

domain size in more complex flows, such as decaying rotating turbulence,[10,22,23] magnetohydrodynamic turbulence,[27] compressible turbulence,[28,29] and turbulent flow with polymer additives.[30]

ACKNOWLEDGMENTS

The authors thank their colleagues Manohar K. Sharma, Roshan J. Samuel, Anando G. Chatterjee, S. Sadhukhan, Shadab Alam, Shashwat Bhattacharya, Ali Asad, and Akanksha Gupta for the useful discussions on freely decaying turbulence. The simulations were performed at the High Performance Computing (HPC) facility of IIT Kanpur, India.

DATA AVAILABILITY

The data that support the findings of this study are available from the corresponding author upon reasonable request.

REFERENCES

[1] P. A. Davidson, *Turbulence: An Introduction for Scientists and Engineers* (Oxford University Press, Oxford, 2004).
[2] A. N. Kolmogorov, "On the degeneration of isotropic turbulence in an incompressible viscous fluid," Dokl. Acad. Nauk SSSR **31**, 319–323 (1941).
[3] G. K. Batchelor, *The Theory of Homogeneous Turbulence* (Cambridge University Press, Cambridge, 1953).
[4] K. R. Sreenivasan, "On the scaling of the turbulence energy dissipation rate," Phys. Fluids **27**, 1048–1051 (1984).
[5] K. R. Sreenivasan, "An update on the energy dissipation rate in isotropic turbulence," Phys. Fluids **10**, 528–529 (1998).
[6] T. Watanabe and K. Nagata, "Integral invariants and decay of temporally developing grid turbulence," Phys. Fluids **30**, 105111 (2018).
[7] S. R. Yoffe and W. D. McComb, "Onset criteria for freely decaying isotropic turbulence," Phys. Rev. Fluids **3**, 104605 (2018).
[8] P. G. Saffman, "Note on decay of homogeneous turbulence," Phys. Fluids **10**, 1349 (1967).
[9] T. Ishida, P. A. Davidson, and Y. Kaneda, "On the decay of isotropic turbulence," J. Fluid Mech. **564**, 455–475 (2006).
[10] P. A. Davidson, N. Okamoto, and Y. Kaneda, "On freely decaying, anisotropic, axisymmetric Saffman turbulence," J. Fluid Mech. **706**, 150–172 (2012).
[11] G. Comte-Bellot and S. Corrsin, "The use of a contraction to improve the isotropy of grid-generated turbulence," J. Fluid Mech. **25**, 657–682 (1966).
[12] P.-Å. Krogstad and P. A. Davidson, "Is grid turbulence Saffman turbulence?," J. Fluid Mech. **642**, 373–394 (2010).
[13] L. Djenidi, M. Kamruzzaman, and R. A. Antonia, "Power-law exponent in the transition period of decay in grid turbulence," J. Fluid Mech. **779**, 544–555 (2015).
[14] M. Sinhuber, E. Bodenschatz, and G. P. Bewley, "Decay of turbulence at high Reynolds numbers," Phys. Rev. Lett. **114**, 034501 (2015).
[15] C. Morize and F. Moisy, "Energy decay of rotating turbulence with confinement effects," Phys. Fluids **18**, 065107 (2006).
[16] L. Skrbek and S. R. Stalp, "On the decay of homogeneous isotropic turbulence," Phys. Fluids **12**, 1997–2019 (2000).
[17] M. Meldi and P. Sagaut, "Turbulence in a box: Quantification of large-scale resolution effects in isotropic turbulence free decay," J. Fluid Mech. **818**, 697–715 (2017).
[18] B. Thornber, "Impact of domain size and statistical errors in simulations of homogeneous decaying turbulence and the Richtmyer-Meshkov instability," Phys. Fluids **28**, 045106 (2016).
[19] A. G. Chatterjee, M. K. Verma, A. Kumar, R. Samtaney, B. Hadri, and R. Khurram, "Scaling of a fast Fourier transform and a pseudo-spectral fluid solver up to 196608 cores," J. Parallel Distrib. Comput. **113**, 77–91 (2018).
[20] M. K. Verma, A. Chatterjee, K. S. Reddy, R. K. Yadav, S. Paul, M. Chandra, and R. Samtaney, "Benchmarking and scaling studies of pseudospectral code Tarang for turbulence simulations," Pramana **81**, 617–629 (2013).
[21] D. Carati, O. Debliquy, B. Knaepen, B. Teaca, and M. K. Verma, "Energy transfers in forced MHD turbulence," J. Turbul. **7**, N51 (2006).
[22] M. K. Sharma, M. K. Verma, and S. Chakraborty, "Anisotropic energy transfers in rapidly rotating turbulence," Phys. Fluids **31**, 085117 (2019).
[23] M. K. Sharma, A. Kumar, M. K. Verma, and S. Chakraborty, "Statistical features of rapidly rotating decaying turbulence: Enstrophy and energy spectra and coherent structures," Phys. Fluids **30**, 045103 (2018).
[24] M. K. Sharma, M. K. Verma, and S. Chakraborty, "On the energy spectrum of rapidly rotating forced turbulence," Phys. Fluids **30**, 115102–115110 (2018).
[25] M. K. Verma, *Energy Trasnfers in Fluid Flows: Multiscale and Spectral Perspectives* (Cambridge University Press, Cambridge, 2019).
[26] M. K. Verma, "Statistical theory of magnetohydrodynamic turbulence: Recent results," Phys. Rep. **401**, 229–380 (2004).
[27] A. Brandenburg and T. Kahniashvili, "Classes of hydrodynamic and magnetohydrodynamic turbulent decay," Phys. Rev. Lett. **118**, 055102 (2017).
[28] R. Samtaney, D. I. Pullin, and B. Kosović, "Direct numerical simulation of decaying compressible turbulence and shocklet statistics," Phys. Fluids **13**, 1415–1430 (2001).
[29] S. Khurshid and D. A. Donzis, "Decaying compressible turbulence with thermal non-equilibrium," Phys. Fluids **31**, 015103 (2019).
[30] P. Perlekar, D. Mitra, and R. Pandit, "Manifestations of drag reduction by polymer additives in decaying, homogeneous, isotropic turbulence," Phys. Rev. Lett. **97**, 264501 (2006).